Paper ID:

ANALYSIS OF MOISTURE-INDUCED DEFORMATION IN BIO-BASED YARNS VIA RH-CONTROLLED X-RAY TOMOGRAPHY

Clément Prunier[1*], Xavier Gabrion[1], Vincent Placet[1]

[1]*Université Marie et Louis Pasteur, SUPMICROTECH, CNRS, Institut FEMTO-ST, Besançon 25000, France*

**clement.prunier@femto-st.fr*

Abstract

This work aims at helping the development of natural fiber yarn for technical and high-performance applications. One of the well-known difficulties for the utilization of natural fiber in technical applications is their sensibility to water. At the yarn scale, hygroscopic swelling of fibers can significantly alter geometrical and morphological properties, thereby affecting key functional characteristics such as fabric breathability. A novel experimental methodology is proposed to characterize the hygroscopic behavior of natural fiber yarns, combining in-situ humidity and temperature conditioning, within an X-ray microtomography environment. This approach enables high-resolution, non-destructive characterization of yarn morphology and dimensional variations along its length under well-controlled environmental conditions across a range of relative humidity levels. The method is demonstrated on a bleached flax yarn, providing insights of its hygroexpansive response. The method allowed to get precise and directional hygroscopic swelling at the yarn scale, obtained through ellipse fitting on cross-sectional scans. The analysis highlights a progressive radial expansion of the yarn, driven by a coupled mechanism involving both fibers swelling and structural rearrangement. Quantitative hygroexpansion coefficients are obtained, along with evidence of slight anisotropy in the hygroexpansion.

Keywords: *Natural fiber; hygroscopic behavior; X-Ray microtomography; in-situ conditioning; yarns*

1 Introduction

With textile industry being the third world's largest polluter, the interest in natural fiber-based textiles is growing. If these fibers are already well developed in common clothing applications, they still struggle to find a place in high-end application, such as sport. One of the reasons is their high sensitivity to moisture, that can be explained by their high content of hemicellulose, a mostly amorphous polysaccharide which displays many hydroxyl groups (OH), favorizing water bonding. The water uptake can reduce the stiffness of the natural fibers, by breaking the hydrogen bonds and occupying the newly free bonding sites [1, 2]. The sorption and desorption cycles can also cause damages within the yarn, and on the interfaces for yarns used within a matrix [3]. With water uptake, natural fiber tends to swell in the transverse direction, a phenomenon called hygroexpansion [2]. This growth can affect the yarn internal structure, but also the textile, affecting its breathability. Hygroexpansion measurements in recent studies have been mostly realized through optical measurements, like digital profile projector [4] or SEM methods [5]. However, these methods only offer a 2D vision of the yarn, and set the hypothesis

of a circular section. Toda et al. [6] showed through X-ray tomography observations that the section was not completely circular, and that the structure of a yarn can show many variations that can affect its reaction to swelling or mechanical loading.
The utilization of X-ray tomography seems therefore to be a good method to get more information about the hygroscopic response of a yarn during water uptake. External conditioning is not well suited to small-scale samples such as yarns, as handling and transfer steps may alter their structure and geometry. In this study, a dedicated conditioning system was developed for integration within a laboratory X-ray microtomography setup, enabling in-situ environmental conditioning and minimizing disturbances to the sample. This system was used to observe the yarn morphology evolution with water uptake, and to determine a directional hygroexpansion coefficient.

2 Methodology and experimental details

2.1 Materials

The studied yarn is a 100 % flax yarn, provided by the company Linificio e Canapificio Nazionale. It has a yarn count (Nm) of 39, and a torsional value of 630 turn/m. A sample of approximately 2 cm long is extracted from the sample, and placed on the sample holder with a point of glue.

2.2 X-Ray microtomography

The experiments are realized on inside a laboratory X-Ray microtomograph EasyTom from RX Solutions, illustrated in Figure 1. The X-ray transmission images (projections) are acquired through a 2530DX detector, with dimensions of 2176 × 1792 pixels². Samples are subjected to 512 images over 360°, in start and stop mode (the interval between each projection is approximately 0.70°). The tube voltage is fixed at 60 keV, and its current is at 83 µA. The framerate is set at 2 images per second, and each projection is obtained after an averaging of 4 images. The acquisition lasts approximately 30 minutes. The volume reconstruction is performed on Xact software (RX Solution) in filtered back-projection, with a voxel size of 1.45 µm, for a total volume of approximately 3.2 × 2.6 × 2.6 mm^3.

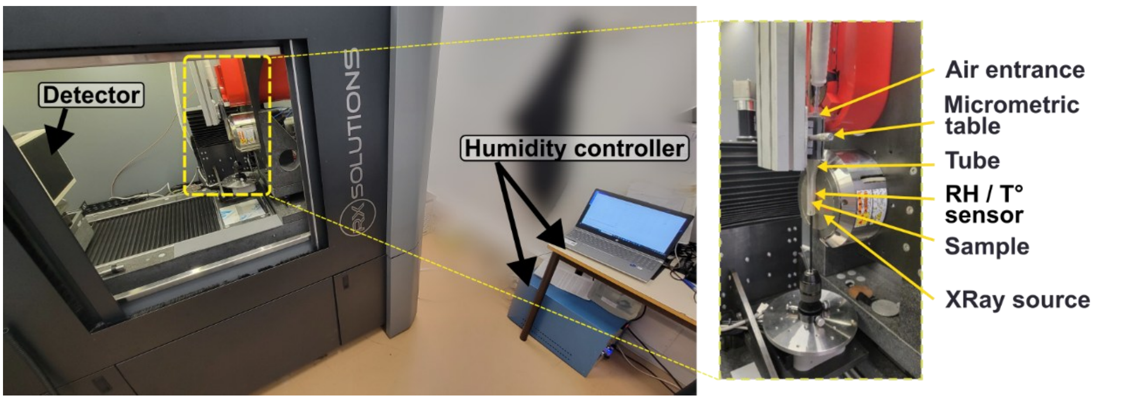

Figure 1. Photo of the in-situ conditioning system inside the micro-tomograph environment.

2.3 RH conditioning

The conditioning is created with a humidity generator (HumiSys by Instruquest), with a transfer line inserted in a tube, which encompass the sample (Figure 1 right). The relative humidity around the sample is monitored through a sensor, placed nearby the sample. Three relative humidity steps are used for this study, respectively 10 %, 50 % and 80 %. A temperature of 20

°C is also maintained in the conditioning tube. Before being inserted in the conditioning system, the sample is kept at ambient humidity and temperature. At each step, the sample is conditioned for a duration significantly exceeding the characteristic time required to reach equilibrium moisture content, previously obtained by Dynamic Vapor Sorption (DVS) measurements made by partners at INRAE. This is made to ensure both hygroscopic equilibrium and the associated morphological and dimensional stabilization. The DVS measurements also provides the moisture content value for the fibers in regard of the conditioning RH value. Multiple scans are performed during the conditioning phase in order to observe the kinetics of stabilization.

2.4 Image processing

After projection, images are processed in an automated code, to extract morphological and dimensional information. The different steps are illustrated in Figure 2. The first part of image processing is realized *via* a macro coded on ImageJ (Figure 2 (a) to (d)). In the first step, each slice is automatically segmented using the triangle method (describes by Zack et al. [7]), leading to the image shown in Figure 2.(b). A first image cleaning step is realized (Figure 2.(c)), with the erasing of outliers, defined as elements with a diameter of 3 px or less. A watershed separation technique is also used to separate fibers and a particle analysis is performed in order to label the fibers (Figure 2. (d)). Finally, the centroid coordinates of each identified object are exported to a python code to be processed. For each slice, the covariance matrix of the point cloud is calculated, allowing to determine a first approximate center and dimensions for the point cloud. The Mahalanobis distance is then computed for each point, providing a metric that accounts for its relative position with respect to the overall orientation of the point cloud ellipse. A first statistical filtering is then performed using a threshold derived from the Chi-square (χ^2) distribution with two degrees of freedom, adopting a 99% confidence level to retain only the points consistent with the main fiber bundle. Then, an ellipse is fitted to the filtered point cloud based on the eigenvalues of its covariance matrix. This ellipse is scaled using a χ^2 threshold corresponding to a 95% confidence level, providing an estimation of the yarn cross-sectional dimensions closer to reality. The width (long axis, in blue on Figure 2 (e) and height (short axis, in red on Figure 2 (e)) of the ellipse are then extracted, and used to calculate its ellipticity rate, based on the formula

$$e = 1 - \frac{h}{w} \qquad (1)$$

With e the ellipticity rate, h the height, and w the width.

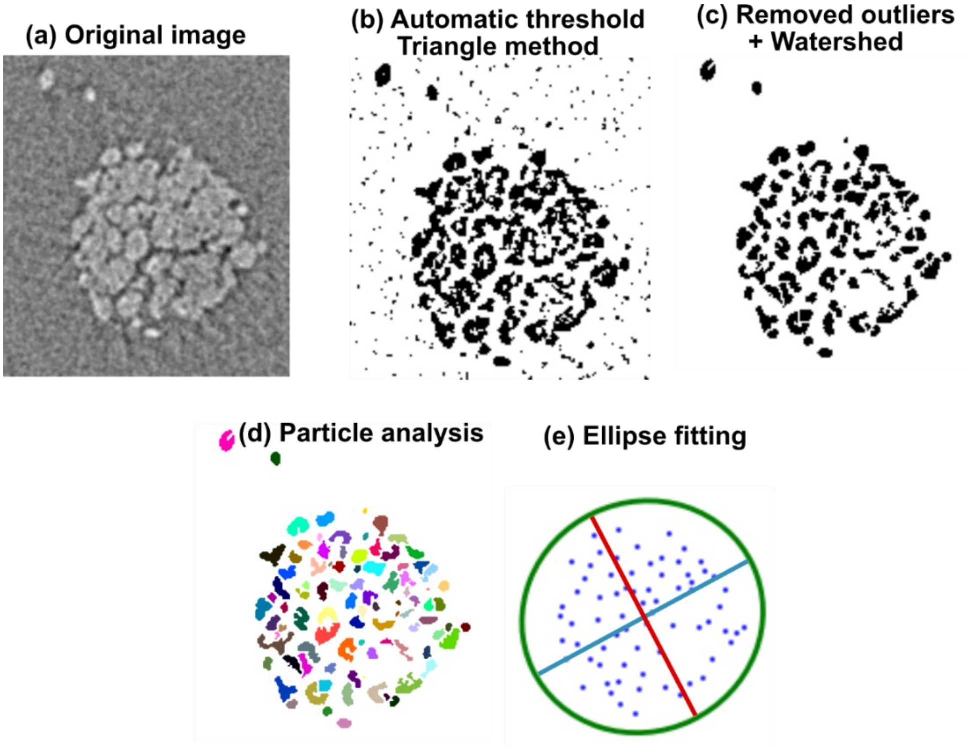

Figure 2. Illustrations of the main steps of the image processing.

3 Results

The evolution of the sample's dimensions for the different relative humidity is plotted in Figure 3. The legend indicates the ambient relative humidity at the moment of the scan, and the time the sample has been conditioned at this humidity before scanning. The height and width of the fitted ellipse are plotted separately, on figure Figure 3 (a) and (b), respectively. This illustration shows the dimensional variability within a single yarn and for simply a 2.5 mm extract, with for example width variation reaching up to 20 %. A first view of the yarn swelling with RH increase can be observed on this figure, particularly by comparing the profiles obtained at 10% RH for 16 hours (red curve) and at 80% RH for 7 hours (black curve). The observed differences indicate a measurable radial expansion of the yarn at higher humidity levels. Also, a slight positional offset appears with increasing RH, which suggests the apparition of structural rearrangements within the yarn, potentially associated with partial untwisting induced by hygroscopic swelling.

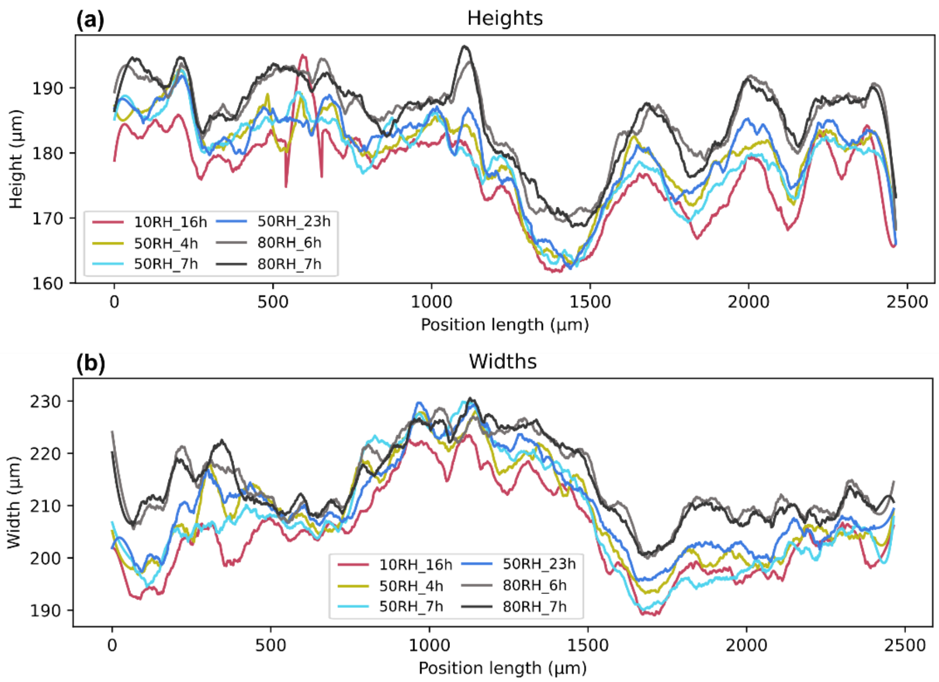

Figure 3. Evolution of the dimensions of the fitted ellipse along yarn lengths. (a) Height (small axis); (b) width (long axis).

The evolution of the mean value along the yarn of each studied dimension in regard to relative humidity variation is illustrated in Figure 4. The width (a) and height (b) evolution shows a clear swelling of the yarn with humidity increase. The width swelling between 10% and 80% RH is of approximately 4.2 %. This increase is slightly higher for the height, with an increase around 4.9 %. This difference causes the slight decrease of the ellipticity ratio, illustrated in Figure 4 (c).

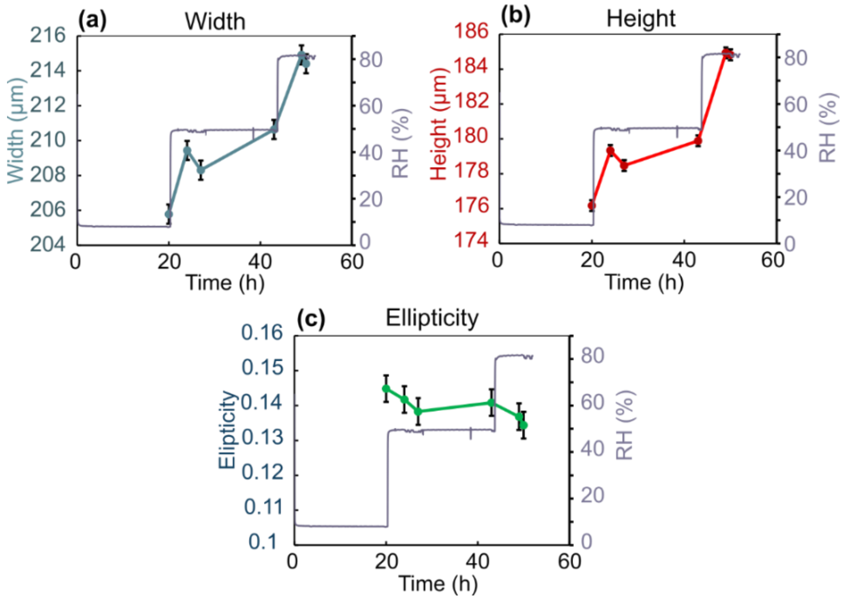

Figure 4. Evolution of the yarn mean dimensions ((a) width, (b) height, (c) ellipticity) and conditioning relative humidity (RH) in function of time.

Figure 5 presents the evolution of the geometrical parameters of the ellipse fitted to the yarn cross-section as a function of moisture content, estimated using the previous DVS measurements. The analysis is reported separately for the principal axes of the ellipse (height and width). The results indicate that the yarn height exhibits an approximately linear hygroexpansion behavior over the investigated moisture range. In contrast, the width shows a slight deviation from linearity, with a tendency toward reduced expansion at higher moisture contents. Nevertheless, the overall behavior remains comparable in both directions, which is consistent with the relatively low ellipticity of the yarn cross-section.

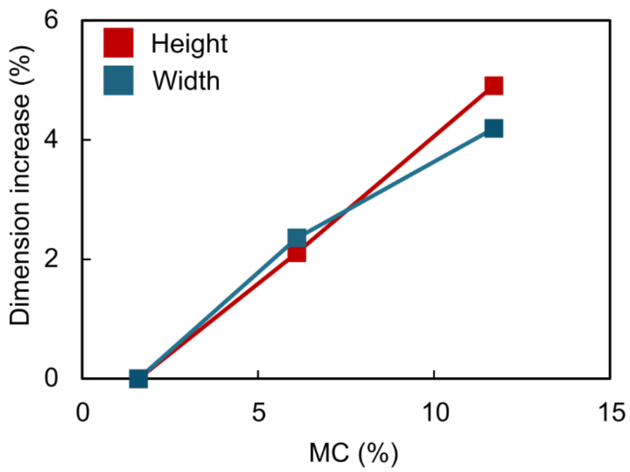

Figure 5. Evolution of the fitted ellipse dimensions with moisture content (MC) in the yarn.

With these values, we can obtain the directional hygroexpansion, β_d, coefficient through the equation

$$\beta_d = \frac{\Delta\varepsilon_d\,(\%)}{\Delta_{MC}(\%)}. \tag{2}$$

With $\Delta\varepsilon_d$ the differential directional hygroscopic deformation, and Δ_{MC} the differential moisture content. The results for the directional hygroexpansion coefficient for the different studied zones are summarized in the Table 1. Values of hygroexpansion coefficients in the width (β_{w}) and height (β_{h}) direction.Table 1.

Table 1. Values of hygroexpansion coefficients in the width (β_{w}) and height (β_{h}) direction.

Zone (RH)	**MC (%)**	$\boldsymbol{\beta_{\mathrm{w}}}$	$\boldsymbol{\beta_{\mathrm{h}}}$
10% - 50%	1.6 - 6.1	0.52	0.47
50% - 80%	6.1 - 11.7	0.32	0.49
10% - 80%	1.6 - 11.7	0.42	0.48

The Figure 6 shows the comparison of a transversal slice of the yarn, after a conditioning at 10 % RH (in red) and 80 % RH (in green). The overlap region between the two images is highlighted in yellow. This comparison reveals that the hygroexpansion of the yarn develops progressively in the radial direction, originating from the core toward the external regions. The observed behavior suggests a coupled mechanism involving both the outward displacement of fibers and their intrinsic transverse swelling.

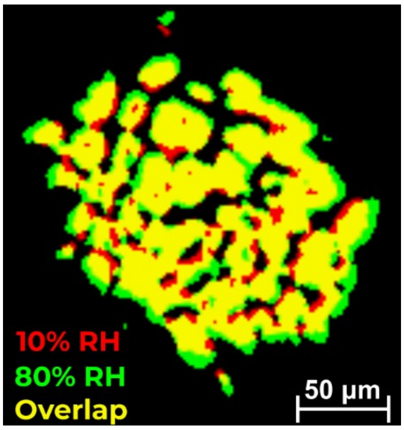

Figure 6. Morphological comparison of a transversal slice of the same position of the flax yarn at 10% RH (in red) and 80% RH (in green). The yellow areas refer to the areas where both images overlap.

4 Conclusion

This work aimed at showing a new methodology to assess the hygroscopic behavior of yarns, with a specificity for natural fiber yarns. It presented a novel in-situ conditioning system to be installed in lab microtomography environment, as well as an innovative post-processing method based on automatized detection of fiber positioning on transversal slices of the yarn, allowing for the determination of a detailed directional dimensional profile of the yarn. The measurements made on a flax yarn allowed to determine quantitative values for directional hygroexpansion coefficients, and that it shows a tendency to linear evolution with moisture content increase. The comparison of slices taken at the same positions highlighted a radial hygroexpansion behavior and a coupling between fiber swelling and displacement. These findings provide valuable input data for multiscale modeling approaches, enabling improved prediction of moisture-induced behavior from the yarn level up to the textile structure. This work introduced a novel methodology to characterize the hygroscopic behavior of yarns, with particular relevance to natural fiber-based yarns. An original in-situ conditioning system, compatible with laboratory X-ray microtomography, was developed to enable controlled humidity and temperature environments. In addition, an advanced post-processing approach based on automated detection of fiber positions in transverse yarn sections was proposed, allowing for the extraction of detailed, directional dimensional profiles along the yarn. Application to a flax yarn provided quantitative values of hygroexpansion coefficients in different directions, revealing a tendency to linear evolution with increasing moisture content. The comparison of cross-sectional images at identical locations showed a predominantly radial hygroexpansion behavior, governed by a coupled mechanism combining fiber swelling and structural rearrangement. These results demonstrate the capability of the proposed approach to capture both global and local morphological changes induced by moisture. The method could be expanded to the measurements of the hygroexpansion coefficient for individual fibers by improving the acquisition resolution and contrast. The generated dataset constitutes a valuable input for multiscale modeling strategies, contributing to improved prediction of hygroscopic behavior from the yarn scale up to the textile structure.

Acknowledgements

This research work is funded by the European Union (Horizon Europe project UPWEARS – 101130741). Views and opinions expressed are however those of the author(s) only and do not necessarily reflect those of the European Union or HADEA. Neither the European Union nor the granting authority can be held responsible for them. The authors thank the MIFHySTO platform (UMLP, France) for providing test equipment. The authors also wish to thank Amelie Moisy and Ilona Anessa at INRAE Nantes for providing us data obtained from DVS measurements.

References

1. Bledzki AK, Reihmane S, Gassan J (1996) Properties and modification methods for vegetable fibers for natural fiber composites. Journal of Applied Polymer Science 59:1329–1336. https://doi.org/10.1002/(SICI)1097-4628(19960222)59:8%253C1329::AID-APP17%253E3.0.CO;2-0

2. Gamstedt EK (2016) Moisture induced softening and swelling of natural cellulose fibres in composite applications. IOP Conf Ser: Mater Sci Eng 139:012003. https://doi.org/10.1088/1757-899X/139/1/012003

3. Perrier A, Touchard F, Chocinski-Arnault L, Mellier D (2017) Influence of water on damage and mechanical behaviour of single hemp yarn composites. Polymer Testing 57:17–25. https://doi.org/10.1016/j.polymertesting.2016.10.035

4. Abida M (2018) Comportement hygroscopique et couplage hygromécanique dans les composites lin / époxy : approche expérimentale multi-échelle et modélisation. Phdthesis, Normandie Université ; École nationale d'ingénieurs de Sfax (Tunisie)

5. Jia T, Wang Y, Dou Y, et al (2019) Moisture Sensitive Smart Yarns and Textiles from Self-Balanced Silk Fiber Muscles. Advanced Functional Materials 29:1808241. https://doi.org/10.1002/adfm.201808241

6. Toda M, Grabowska K, Ciesielska-Wróbel I (2017) Application of micro-computed tomography (micro-CT) to study unevenness of the structure of yarns. Textile Research Journal 87:351–368. https://doi.org/10.1177/0040517516629149

7. Zack GW, Rogers WE, Latt SA (1977) Automatic measurement of sister chromatid exchange frequency. J Histochem Cytochem 25:741–753. https://doi.org/10.1177/25.7.70454